

Interferometric tunability of absorption

Vittorio Giovannetti¹, Seth Lloyd², Lorenzo Maccone³

¹*NEST-CNR-INFM and Scuola Normale Superiore,
Piazza dei Cavalieri 7, I-56126, Pisa, Italy.*

²*MIT, Research Laboratory of Electronics and Dept. of Mechanical Engineering,
77 Massachusetts Avenue, Cambridge, MA 02139, USA.*

³*QUIT - Quantum Information Theory Group, Dip. Fisica "A. Volta",
Univ. di Pavia, via Bassi 6, I-27100 Pavia, Italy.*

Abstract: We propose an interferometric setup that permits to tune the quantity of radiation absorbed by an object illuminated by a fixed light source. The method can be used to selectively irradiate portions of an object based on their transmissivities or to accurately estimate the transmissivities from rough absorption measurements.

© 2006 Optical Society of America

OCIS codes: (120.3180) Interferometry; (300.1030) Absorption; (170.0110) Imaging systems

References and links

1. A. Elizur and L. Vaidman, "Quantum mechanical interaction-free measurements," *Found. Phys.* **23**, 987-997 (1993); L. Vaidman, "On the realization of interaction-free measurements," *Quantum Opt.* **6**, 119 (1994).
2. P. Kwiat, H. Weinfurter, A. Zeilinger, "Quantum Seeing in the Dark," *Sci. Am.* **275**, 72-77 (1996); P. Kwiat, H. Weinfurter, T. Herzog, A. Zeilinger, M. A. Kasevich, "Interaction-Free Measurement," *Phys. Rev. Lett.* **74**, 4763-4767 (1995).
3. A. G. White, J. R. Mitchell, O. Nairz, and P. G. Kwiat, "«Interaction-free» imaging," *Phys. Rev. A* **58**, 605-613 (1998).
4. P. Kwiat, "Experimental and theoretical progress in interaction-free measurements," *Physica Scripta* **T76**, 115-121 (1998).
5. P. Facchi, Z. Hradil, G. Krenn, S. Pascazio, and J. Řeháček, "Quantum Zeno tomography," *Phys. Rev. A* **66**, 12110 (2002).
6. S. Inoue and G. Björk, "Experimental demonstration of exposure-free imaging and contrast amplification," *J. Opt. B: Quantum Semiclass. Opt.* **2**, 338-345 (2000).
7. J.-S. Jang, "Optical interaction-free measurement of semitransparent objects," *Phys. Rev. A* **59**, 2322-2329 (1999).
8. Rigorously speaking, the transformation $\beta_{n+1} \rightarrow \sqrt{\eta}\beta_{n+1}$ does not correspond to the linear mapping $|\beta_{n+1}\rangle \rightarrow |\sqrt{\eta}\beta_{n+1}\rangle$ but to its density matrix counterpart: $|\beta_{n+1}\rangle\langle\beta_{n+1}| \rightarrow |\sqrt{\eta}\beta_{n+1}\rangle\langle\sqrt{\eta}\beta_{n+1}|$. The latter accounts for decoherence effect, whereas the former does not. Since in our analysis we are always dealing with factorized states, the two transformations coincide for us.
9. This effect can be explained intuitively as follows. If the object is transparent, at the first round trip a small amount of radiation leaks into the R modes, at the second round trip a higher amount leaks there and so on constantly increasing through constructive interference until all the radiation moves into such modes after $N = \pi/\phi$ round trips. If, instead, the object is opaque, the little radiation that has leaked into the R modes at the first round trip is absorbed and does not contribute to the constructive interference that would draw more radiation into these modes at the second round trip. As a result very little radiation transfers and most of it remains in the L modes.

1. Introduction

When an object is illuminated, it will absorb radiation proportionally to its absorption coefficient: Darker portions of the object will absorb more light than more transparent ones. Is there a way around this? In this paper we analyze a setup which uses classical light sources

(i.e. coherent beams) and permits to easily tune the quantity of a light absorbed by an object independently on its transparency, by appropriately tuning an interferometer phase. With the same setup, high efficiency measurements of the absorption coefficient can be performed via a feedback mechanism. The only underlying assumption is that the object introduces a negligible dephasing into a probe beam. Since we can employ quasi-monochromatic light, this assumption is met in a variety of systems. Moreover, in the case of objects that have a homogeneous phase image, the dephasing can be easily compensated with the interferometer phase.

Our proposal draws inspiration from the so called “interaction-free-measurement” setups, where a partially transparent object can be discriminated from a totally transparent one with asymptotically negligible radiation absorption [1, 2, 3, 4, 5]. Even though such proposals were originally based on single-photon light pulses, analogous results have been obtained also with classical light [6, 7].

The layout of the paper follows. We start by describing the proposed interferometric setup. We show how the absorption peak can be tuned and we analyze the irradiation selectivity. We then give the protocol for high efficiency estimation of η . We conclude by analyzing inhomogeneous objects, which incorporate different transmissivities. Since the process does not involve any quantum effects (such as entanglement or squeezing) one could also analyze it in terms of a classical theory of radiation, instead of the quantum formalism we use here for rigor.

2. The apparatus

The proposed apparatus is a modification of the experimental setup of Ref. [7]. It is obtained by concatenating a collection of N Mach-Zehnder (MZ) interferometers and is depicted in Fig. 1. Initially a coherent state $|\alpha\rangle$ enters through one interferometer port (associated with the annihilation operator a_0), and no photons enter from the other port (associated with the annihilation operator b_0). As shown in Fig. 1, after each MZ, one of the two emerging beams (the R beam) is focused on the object. Then the two beams are recombined at the input port of the next MZ. After N of such steps, the radiation leaves the apparatus at the N th interferometer outputs a_N and b_N . As we will show, appropriately tuning the interferometers phase ϕ and the number N of MZs it is possible to choose the value of the transmissivity η that will absorb the most radiation in the object. The transmissivity η of an object is the probability that a single photon will pass through it or, equivalently, the percentage of the transmitted intensity of an impinging coherent beam. Note that an apparatus employing a *single* MZ which is crossed N times by the light can also be employed, where N can be controlled by appropriately tilting one of the interferometer mirrors [7] or by using an acousto-optics switch.

The input-output relations of the interferometer can be obtained observing that when two coherent states $|\alpha_n\rangle$ and $|\beta_n\rangle$ impinge, respectively, into the input ports a_n and b_n of the n -th MZ (see Fig. 2), the corresponding outputs at ports a_{n+1} and b_{n+1} are still coherent states of amplitudes α_{n+1} and β_{n+1} , given by

$$\begin{pmatrix} \alpha_{n+1} \\ \beta_{n+1} \end{pmatrix} = S \begin{pmatrix} \alpha_n \\ \beta_n \end{pmatrix}, \quad (1)$$

with

$$S = e^{i\phi/2} \begin{pmatrix} \cos(\phi/2) & i \sin(\phi/2) \\ i \sin(\phi/2) & \cos(\phi/2) \end{pmatrix}, \quad (2)$$

where ϕ is the interferometer phase. The output a_n is directly fed into a port of the MZ number $n + 1$, while the output b_n first passes through the object and then enters the other port of the same MZ. Since the object absorbs each photon with a probability η without introducing any phase factor, its action on the input coherent state $|\beta_{n+1}\rangle$ can be modeled as a beam splitter

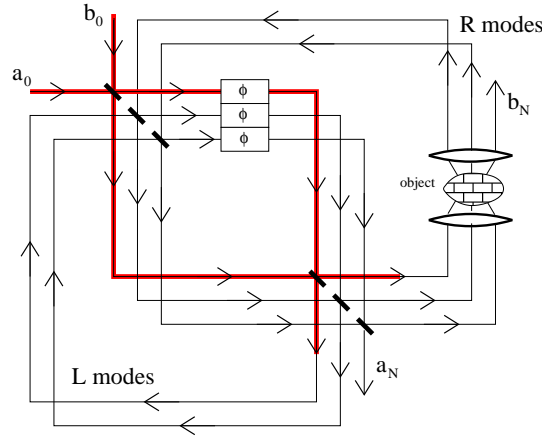


Fig. 1. Proposed apparatus. It consists of N Mach-Zehnder (MZ) interferometers concatenated so that the output ports of the n th MZ is fed into the input ports of the successive one (for the sake of clarity the first interferometer is graphically enhanced). All interferometers act on the radiation with the same phase shift ϕ . The object to be irradiated is placed outside the MZs and it interacts only with the R beams. Initially the radiation enters from the input a_0 . After N round trips, it exits through the outputs a_N and b_N .

with transmissivity η that couples the input radiation to a vacuum state and then discards one of the two outputs. As a result the state $|\beta_{n+1}\rangle$ is transformed into a coherent state of reduced amplitude $\sqrt{\eta}\beta_{n+1}$ [8]. Thus, in the presence of the absorber, the amplitudes α_{n+1} and β_{n+1} of the coherent states at the input of the MZ interferometer number $n + 1$ is given by

$$\begin{pmatrix} \alpha_{n+1} \\ \beta_{n+1} \end{pmatrix} = S(\eta) \begin{pmatrix} \alpha_n \\ \beta_n \end{pmatrix}, \quad (3)$$

where

$$S(\eta) = e^{i\phi/2} \begin{pmatrix} \cos(\phi/2) & i \sin(\phi/2) \\ i\sqrt{\eta} \sin(\phi/2) & \sqrt{\eta} \cos(\phi/2) \end{pmatrix}. \quad (4)$$

Iterating Eq. (3) N times we can express the amplitude of the coherent states emerging from the whole apparatus as

$$\begin{pmatrix} \alpha_N \\ \beta_N \end{pmatrix} = S^N(\eta) \begin{pmatrix} \alpha_0 \\ 0 \end{pmatrix}. \quad (5)$$

Some examples of such evolution are given in Fig. 3, and an analytic solution can be obtained by diagonalizing $S(\eta)$ [7]. The light absorbed by the object is given by

$$I_{\text{ab}} = |\alpha_0|^2 - (|\alpha_N|^2 + |\beta_N|^2) \equiv r |\alpha_0|^2, \quad (6)$$

i.e. the input intensity $|\alpha_0|^2$ minus the total output intensity $|\alpha_N|^2 + |\beta_N|^2$. The quantity r is a complicated function of N , ϕ and η which can be explicitly computed from Eq. (5). It measures the “effective” absorption constant of the object.

3. Discussion

The possibility of changing the absorption of the illuminated object from its natural value $1 - \eta$ to an effective value $r \simeq 0$ allows one to determine the presence of a completely opaque object

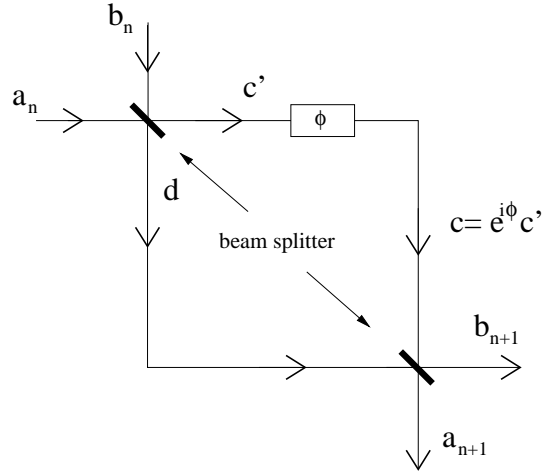


Fig. 2. Mach-Zehnder interferometer constituting the n th element in the Mach-Zehnder sequence in the apparatus of Fig 1. The first of the two 50-50 beam splitters transforms the input annihilation operators a_n , b_n into $c' = (a_n + b_n)/\sqrt{2}$ and $d = (b_n - a_n)/\sqrt{2}$ respectively. The second beam splitter transforms the annihilation operators c and d into $a_{n+1} = (c + d)/\sqrt{2}$ and $b_{n+1} = (d - c)/\sqrt{2}$.

(i.e. $\eta = 0$) with only an asymptotically small fraction of the input radiation being absorbed [7, 3, 4, 5, 6]. Consider Eq. (5) for $\eta = 1$ (e.g. completely transparent object) and $\eta = 0$ (e.g. completely opaque object). In these cases simple analytical solutions can be obtained yielding

$$\alpha_N = \alpha_0 e^{iN\phi/2} \cos(N\phi/2) \quad (7)$$

$$\beta_N = i\alpha_0 e^{iN\phi/2} \sin(N\phi/2), \quad (8)$$

for $\eta = 1$, and

$$\alpha_N = \alpha_0 e^{iN\phi/2} \cos^N(\phi/2) \quad (9)$$

$$\beta_N = 0, \quad (10)$$

for $\eta = 0$. By choosing $\phi = \pi/N$, from Eqs. (8) and (10), it is immediate to see that all radiation exits from the b_N -port if $\eta = 1$ and that most of the radiation (asymptotically all of it for $N \rightarrow \infty$) exits from the a_N -port if $\eta = 0$ [9]. In both cases the light absorption is minimal (i.e. exactly null in the first case and asymptotically null in the second one). Nonetheless they can be discriminated by simply looking from which interferometer ports (e.g. a_N or b_N) the light emerges.

The possibility of controlling the effective absorption r of the object by changing the interferometer parameters is evident from Fig. 4 where we plot r as a function of the transmissivity η for different values of ϕ (choosing again $N = \pi/\phi$): The function r exhibits a peak for $\eta = \eta_{max}$ which increases from $\eta_{max} \sim 0$ to $\eta_{max} \sim 1$ as ϕ decreases. This effect can be explained intuitively as follows. For small values of ϕ (i.e. high values of N) little radiation is leaked into the R modes at every round trip with the exception of the case when η is high. On the contrary, for small values of N (i.e. large values of ϕ) a larger amount of radiation is leaked into the R modes at every round trip, so that the absorption peak moves to lower values of η . The dependence of the absorption peak maximum as a function of ϕ and N is depicted in Fig. 5, left. This graph also shows the values of η_{max} that can be attained in practice: it can be accurately fine-tuned

only for $\eta_{max} \gtrsim 0.5$ since only few discrete values of η_{max} are achievable for low N , whereas high $\eta_{max} \sim 1$ requires large N , which can be difficult to achieve practically. Finally, the selectivity of the absorption, i.e. the width of the effective absorption curve r as a function of η (see Fig. 4), is not constant when ϕ is varied: The value of the width-at-half-maximum is smaller for absorption curves peaked at $\eta_{max} \simeq 0,1$ and larger for $\eta_{max} \simeq 0.5$. In the limit $\phi \rightarrow 0$ the r -curve becomes a very narrow spike peaked just below $\eta = 1$.

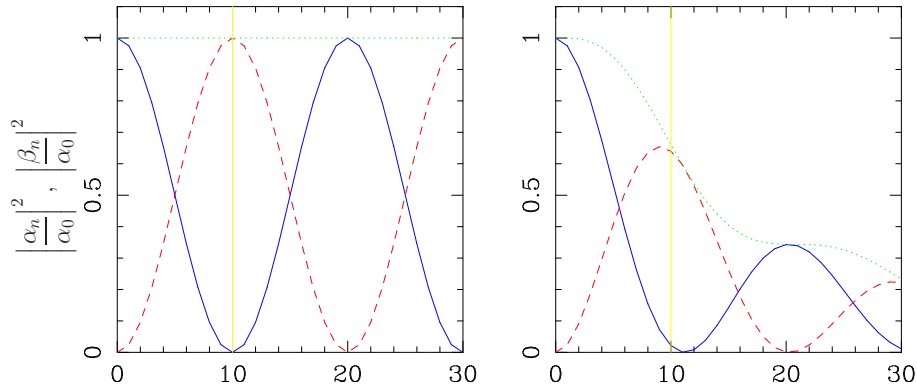


Fig. 3. Plot of the (rescaled) output amplitudes of the n th MZ interferometer $|\alpha_n/\alpha_0|^2$ in the a -modes at L (continuous line) and $|\beta_n/\alpha_0|^2$ in the b -modes at R (dashed line). Initially all the radiation is in mode a_0 , but, as the evolution progresses, more and more radiation is transferred to the b -modes, until (for $n = \pi/\phi$) the radiation is entirely transferred. Here $\phi = \pi/10$ so that the total transfer occurs for $n = 10$ (vertical line). Left: The object is completely transparent ($\eta = 1$), so that the total energy (dotted line) is constant; Right the object is semi-transparent ($\eta = .9$), so that the total energy decreases as the evolution progresses.

4. High precision η -measurements

Our scheme can be easily adapted to high precision estimation of the absorption coefficient, starting from low-quality measurements of the absorption r . [The main idea is revealed by the lower right graph of Fig. 4.] The required iterative procedure is composed by the following steps: i) start by roughly estimating η through an absorption measurement and set the interferometer phase so that the r curve has a steep slope corresponding to such value of η ; ii) perform another absorption measurement and estimate a better value of η ; iii) again tune the interferometer phase, and so on. Since the absorption curve r for the values of $\eta \sim 1$ can be very steep, a very good estimate of these η s can be achieved even when the measurement of r contains a large error Δr (see Fig. 4). Notice that the high values of $\eta \sim 1$ are the hardest to estimate reliably without strongly irradiating the object, since they are associated to the region of least transparency.

5. Inhomogeneous samples

In deriving Eq. (3) we implicitly assumed that η is constant, i.e. that we employ a spatially homogeneous object with uniform absorption within the waist of the light beams crossing it. Instead, if it has spatially inhomogeneous absorption, we can still use Eq. (3) to describe the ab-

sorption of “portions” of the incoming beam. In fact, in the limit in which the scale of the spatial inhomogeneities is much larger than the wavelength λ of the source light, the diffraction of the propagating beam induced by these inhomogeneities can be neglected. In this regime the illuminating beam can be effectively decomposed in independent “sub-beams” of the wavelength λ and interacting independently with the different portions of the object. A typical example is when one performs imaging of a macroscopic object. Controlling the interferometer parameters we can then selectively choose which portion will absorb the most of the input radiation by appropriately shifting the position of the absorption peak of r .

Explicitly, to selectively irradiate an inhomogeneous sample one thus needs to: i) estimate the transmissivity of the various portions of the sample by conventional imaging techniques, identifying the transmissivity $\bar{\eta}$ of the region that needs irradiation; ii) tune the phase $\phi = \pi/N$ so that the absorption is maximized for $\bar{\eta}$.

S. L. acknowledges financial support by ARDA, DARPA, ARO, AFOSR, NSF, and CMI; V. G. was in part supported by the EC under contract IST-SQUBIT2 and by the Quantum Information research program of Centro di Ricerca Matematica Ennio De Giorgi of Scuola Normale Superiore; L. M. acknowledges financial support by the Ministero Italiano dell'Università e della Ricerca (MIUR) through FIRB (bando 2001) and PRIN 2005.

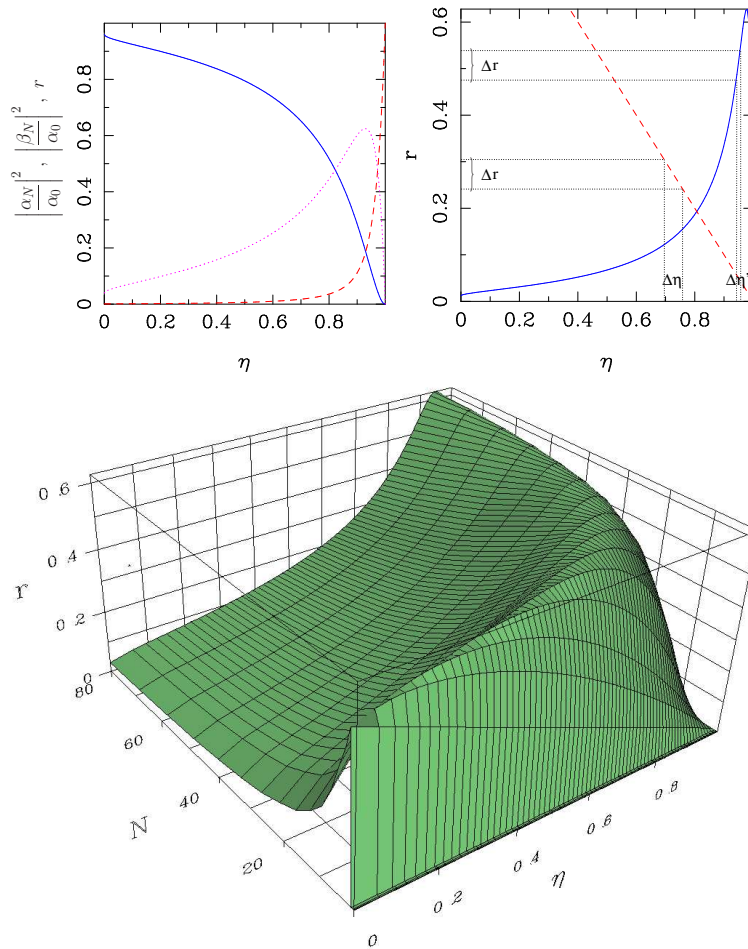


Fig. 4. Above left: Plot of the (rescaled) apparatus output amplitudes $|\alpha_N/\alpha_0|^2$ at the output a_N (continuous line) and $|\beta_N/\alpha_0|^2$ at b_N (dashed line) as a function of the transmissivity η of the object with $\phi = \pi/60$. For $\eta = 1$ (total transparency) all the output radiation is at b_N , whereas for $\eta = 0$ (total absorption) all the output radiation is at a_N and a small amount of radiation has been absorbed. The absorbed radiation is proportional to the effective absorption constant r , defined in Eq. (6), which is depicted by the dotted lines. Above right: Plot of the absorption r only, in the case $\phi = \pi/200$. This plot illustrates how the setup can be used to measure the absorption coefficient η by measuring r , attaining a higher precision than with a direct measure (in which case the absorption is given by the dashed line): Starting from the same uncertainty Δr in the measurement of r with our procedure we can obtain a lower uncertainty $\Delta\eta'$ in the measurement of η than the one, $\Delta\eta$, obtainable from a direct measurement. Below: Plot of r as a function of η and $N = \pi/\phi$. Notice how the absorption peak shifts as a function of ϕ . The absorption peak moves to higher η for decreasing ϕ .

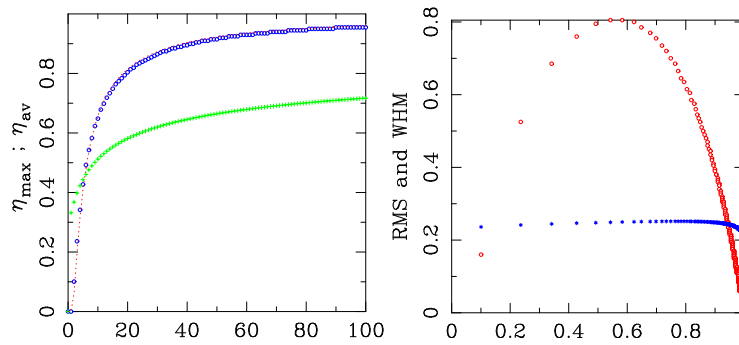


Fig. 5. Left: Maximum η_{max}^N (circles) and average value η_{av} (squares) of the absorption peak r of Fig. 4 as a function of $N = \pi/\phi$. (The maximum and the average follow different evolutions because of the asymmetry in the absorption curves). Increasing N (i.e. decreasing ϕ), the maximum in the absorption peak moves to higher values of η . The graph also details which are the actual values of η that can be achieved through the proposed setup as a function of N . The dotted line is the function $[(N-1)/N]^4$ that gives a good interpolation of the peak evolution. Right: Selectivity in the irradiation as a function of the transmissivity peak. The width of the peaks of the dotted line in Fig. 4 is not uniform. Here we plot the Root Mean Square (stars) and the width at half maximum (circles) of the absorption curve as a function of the absorption curve maximum. Notice that the RMS is almost constant over the whole range.